γδ T Cells Kill *Plasmodium falciparum* in a Granzyme- and Granulysin-Dependent Mechanism during the Late Blood Stage

Maria Andrea Hernández-Castañeda,* Katharina Happ,* Filippo Cattalani,* Alexandra Wallimann,* Marianne Blanchard,* Isabelle Fellay,* Brigitte Scolari,* Nils Lannes,* Smart Mbagwu,* Benoît Fellay,† Luis Filgueira,* Pierre-Yves Mantel,* and Michael Walch*

***Plasmodium* spp., the causative agent of malaria, have a complex life cycle. The exponential growth of the parasites during the blood stage is responsible for almost all malaria-associated morbidity and mortality. Therefore, tight immune control of the intraerythrocytic replication of the parasite is essential to prevent clinical malaria. Despite evidence that the particular lymphocyte subset of γδ T cells contributes to protective immunity during the blood stage in naive hosts, their precise inhibitory mechanisms remain unclear. Using human PBMCs, we confirmed in this study that γδ T cells specifically and massively expanded upon activation with *Plasmodium falciparum* culture supernatant. We also demonstrate that these activated cells gain cytolytic potential by upregulating cytotoxic effector proteins and IFN-γ. The killer cells bound to infected RBCs and killed intracellular *P. falciparum* via the transfer of the granzymes, which was mediated by granulysin in a stage-specific manner. Several vital plasmodial proteins were efficiently destroyed by granzyme B, suggesting proteolytic degradation of these proteins as essential in the lymphocyte-mediated death pathway. Overall, these data establish a granzyme- and granulysin-mediated innate immune mechanism exerted by γδ T cells to kill late-stage blood-residing *P. falciparum*. *The Journal of Immunology*, 2020, 204: 1798–1809.**

Malaria remains one of the major health problems that challenge developing countries. More than 200 million people are annually infected worldwide with *Plasmodium* spp. parasites (1). In the human host, *Plasmodium* spp. have a complex life cycle, including a liver and blood stage. However, it is accepted that clinical malaria is caused by the intraerythrocytic replication of the parasites. These replication cycles start with the release of merozoites from the liver into the blood stream, followed by a rapid invasion of uninfected RBCs. Merozoites differentiate into a ring form that grows into a trophozoite. In the subsequent schizont stage, the nucleus undergoes multiple divisions to give rise to several daughter merozoites. These repeated cycles of invasion, replication, and egress from RBCs lead to exponential growth of the parasites in the blood, responsible for almost all the clinical symptoms of malaria and the associated morbidity and mortality. Therefore, to efficiently prevent malaria pathogenesis and progression toward severe disease, tight control of parasitemia is essential (2).

Protective immune responses to blood-stage malaria are highly complex, requiring the interplay of innate and adaptive mechanisms of humoral (3) and cellular immunity (4, 5). Abs inhibit parasite invasion at several levels, such as through phagocytosis and complement activation (6, 7). However, less is known about cytotoxic immune cell mechanisms during the blood stage. A particular subset of T lymphocytes, bearing the γδ TCR, has been demonstrated to be of importance in defending the host against a broad range of pathogens (8). In patients suffering from *Plasmodium falciparum* infection, γδ T cells, particularly cells bearing the Vγ9Vδ2 TCR (9), expand massively in the peripheral blood (10, 11). Nevertheless, their inhibitory mechanisms remain ill defined (12).

Cytotoxic lymphocytes kill infected or malignantly transformed cells by the release of their cytotoxic granule content. Target cell death is mediated by cytotoxic serine proteases, the granzymes (Gzms), that are delivered into the target cell by the pore-forming protein perforin (PFN) (13). Cytotoxic granules of some mammals contain another cytolytic protein, granulysin (GNLY), that preferentially targets prokaryotic cholesterol-poor membranes, such as of bacteria, fungi, and parasites (14, 15). In line with that, it has

*Anatomy Unit, Department of Oncology, Microbiology and Immunology, Faculty of Science and Medicine, University of Fribourg, 1700 Fribourg, Switzerland; and †Cantonal Hospital of Fribourg, 1752 Villars-sur-Glâne, Switzerland

ORCIDs: 0000-0002-7151-3546 (M.A.H.-C.); 0000-0001-8392-0715 (F.C.); 0000-0001-6755-3679 (A.W.); 0000-0002-2926-6182 (N.L.); 0000-0003-4297-6303 (S.M.); 0000-0001-5270-629X (B.F.); 0000-0001-9526-9309 (P.-Y.M.); 0000-0001-7284-3291 (M.W.).

Received for publication June 26, 2019. Accepted for publication January 15, 2020.

This work was supported by the Swiss National Science Foundation (Grant 310030_169928 to M.W.), the Bangerter-Rhyner-Foundation (to M.W. and P.-Y.M.), and the Research Fund of the University of Fribourg (to M.W.).

Address correspondence and reprint requests to Dr. Pierre-Yves Mantel or Prof. Michael Walch, Department of Oncology, Microbiology and Immunology, Faculty of Science and Medicine, University of Fribourg, PER03.I.15, Route Albert Gockel 1, 1700, Fribourg, Switzerland (P.-Y.M.) or Department of Oncology, Microbiology and Immunology, Faculty of Science and Medicine, University of Fribourg, PER03.I.14, Route Albert Gockel 1, 1700, Fribourg, Switzerland (M.W.). E-mail addresses: pierre-yves.mantel@unifr.ch (P.-Y.M.) or michael.walch@unifr.ch (M.W.)

Abbreviations used in this article: BCECF-AM, 2,7-bis(2-carboxyethyl)-5(6)-carboxyfluorescein acetoxymethyl ester; CMA, concanamycin A; DCI, 3,4-dichloroisocoumarin; GNLY, granulysin; Gzm, granzyme; GzmB, Gzm B; HCT, hematocrit; hu, hemolytic unit; iRBC, infected RBC; MCM, malaria culture medium.

been demonstrated that the antiplasmodial activity of γδ T cells depended on GNLY (16, 17).

We have recently discovered that cytotoxic lymphocytes (by the concerted action of PFN, GNLY, and the Gzms) kill intracellular bacteria (18) and certain unicellular parasites, such as *Trypanosoma cruzi* (19). In this study, we followed up on this line of research and addressed the question of how γδ T cells restrict the growth of blood-residing *P. falciparum*.

Materials and Methods

Parasites

Cultures of the 3D7 strain *P. falciparum* were used in the experiments. Parasites were cultured in human A^+ RBCs (obtained from healthy volunteers) in malaria culture medium (MCM) composed of RPMI 1640 (25 mM HEPES, low bicarbonate, no glutamine; Sigma-Aldrich) supplemented with 1% heat-inactivated human serum, Albumax II (Life Technologies), gentamicin (Sigma-Aldrich), 20% glucose, and hypoxanthine, as previously described (20, 21). The parasites were maintained at 37˚C in 5% CO_2, 5% O_2, and 90% N_2. Hematocrit (HCT) was adjusted to 2%, except where specified otherwise.

Stage-specific parasite enrichments

An enrichment of ring stages was achieved as previously described (22). Briefly, a culture with high proportion of later-stage parasites and with parasitemia between 3 and 10% was centrifuged at 240 × *g* for 10 min, supernatant was removed, and pellet was resuspended in 20 vol of 0.5% gelatin in RPMI and incubated at 37˚C for 30–60 min. After the incubation, the supernatant was transferred to a fresh tube, centrifuged at 240 × *g* for 4 min, and supernatant was discarded. The pellet was washed twice, and HCT was adjusted to 0.5% by adding appropriate volume of MCM and incubated at 37˚C in 5% CO_2 for 18–20 h.

For experiments requiring late stages (trophozoites and schizonts), a culture with high proportion of ring stage and with parasitemia >5% was centrifuged at 1800 rpm for 4 min, and supernatant was removed. Pellet was treated with 5% D-sorbitol (Sigma-Aldrich) for 10 min at 37˚C. After the incubation, the culture was centrifuged at 1800 rpm for 4 min, supernatant was discarded, pellet was washed twice, and HCT was adjusted to 0.5% by adding appropriate volume of complete medium and incubated at 37˚C in 5% CO_2 for 18–20 h.

Purification of cytotoxic effector molecules

Native GNLY, Gzm B (GzmB), and PFN were purified from the human NK cell line YT-Indy as described previously (23–25). The hemolytic activity of PFN was determined using serial dilutions in assay buffer (10 mM HEPES, 0.15 M NaCl, and 0.1% BSA, pH 7.5) that were incubated with an equal volume of 0.2% human RBCs in assay buffer containing 5 mM $CaCl_2$ at 37˚C for 20 min in round-bottom microtiter plates (Nunc, Rochester, NY). After the incubation, plates were centrifuged at 400 × *g* for 3 min, and the supernatants were transferred to a second flat-bottom plate. The hemoglobin released into the supernatant was detected with a microplate reader at a wavelength of 405 nm. One hemolytic unit (hu) was defined as the amount resulting in 50% lysis of 0.1% RBCs in a volume of 0.2 ml.

For some experiments, GzmB was fluorescently labeled using the Alexa Fluor 488 Microscale Protein Labeling Kit (Thermo Fisher Scientific) following manufacturer's recommendations.

γδ T cell expansion and activation

γδ T cells were generated from PBMC isolated from whole blood of healthy donors (blood bank, Bern, Switzerland) by Ficoll-Paque PLUS (GE Healthcare) density centrifugation. PBMCs were cultured in H10 (RPMI supplemented with 10% heat-inactivated human serum and 1% antibiotic/antimycotic solution [Thermo Fisher Scientific]) for 1 h at 37˚C. After the incubation, the nonadherent suspension cells were collected and further cultured in H10 supplemented with a 1/50 dilution of infected RBC (iRBC) culture supernatants (mixed stages, 10% parasitemia) + 100 U/ml recombinant human IL-2 (Miltenyi) for 14 d (26). As controls for the activation conditions, the supernatant of non-iRBCs (cultured using the same protocol for iRBCs) + IL-2 and IL-2 alone were used. The cells were diluted and supplemented with fresh supernatant/IL-2 every 3–4 d. For some experiments, the iRBC supernatant was size fractionated by passing through a spin filter column (Amicon Ultra, 10-kDa cutoff; Merck). In addition, to exclude endotoxin contamination, iRBC supernatants were sporadically assessed for LPS (ToxinSensor Chromogenic LAL Endotoxin Assay Kit; GenScript). For indicated experiments, after 7 d of activation, the effector cell population was enriched for γδ T cells using a MACS kit (Positive MACS Selection; Miltenyi) following manufacturer's recommendations, routinely yielding a cell purity of >95%. To get rid of the bound Abs after the MACS purification, the γδ T cells were further expanded with culture supernatant and IL-2 for another 6 d before their use in reinvasion assays. Cell purity after the further expansion phase was reassessed by flow cytometry (see Fig. 3D).

γδ T cell phenotypization

For phenotyping, cells were stained with fluorescently conjugated anti-CD45 and anti-CD3 (for flow cytometry gating) as well as with anti-αβ−TCR, γδ−TCR, anti-CD56 Abs (all BD), and/or Vδ2-TCR (Miltenyi) on ice before analysis by flow cytometry (MACSQuant; Miltenyi). Wherever available, appropriate isotype control Abs were used to establish the staining protocols and test the specificity of the primary Abs. For cytometry assays, cell viability was assessed with Zombie Aqua (BioLegend). For intracellular cytokine assessment, cells were pretreated with the cell activation mixture (BioLegend) containing brefeldin (5 μg/ml), PMA (81 μM), and ionomycin (1.34 μM) for 4 h at 37˚C before staining for surface markers on ice. After fixation and permeabilization (Fixation/Permeabilization Kit; BD Biosciences), the cells were stained with an anti–IFN-γ Ab (BioLegend) for assessment by flow cytometry, and cell viability was assessed using Zombie Aqua (BioLegend). For imaging, the specimens were counterstained with DAPI (1 μg/ml; Sigma-Aldrich) or with Hoechst dye (1 μg/ml; Sigma-Aldrich), mounted in Vectashield (Vector Laboratories), and analyzed by confocal microscopy (SP5; Leica). The IFN-γ levels were assessed by ELISA (IFN-γ dual kit; R&D Systems) following manufacturer's recommendations. The dilutions of the supernatants before the ELISA, including the splitting dilutions during the expansion and activation of the cells, were respected in the calculation of IFN-γ levels to reflect the total production of the cytokine during the activation. To confirm their cytolytic potential, the cells were stained with fluorescently conjugated anti-GzmB, GNLY, and PFN Abs (BD Biosciences) using a kit for intracellular protein staining (Fixation/Permeabilization Kit; BD Biosciences); counterstained with DAPI; mounted in Vectashield; and assessed by confocal microscopy. Additionally, their cytotoxic potential was tested using K562 cells in 2,7-bis(2-carboxyethyl)-5(6)-carboxyfluorescein acetoxymethyl ester (BCECF-AM; Sigma-Aldrich) release assays, as described (27, 28). As controls, killer cells were pretreated with 3,4-dichloroisocoumarin (DCI) (25 μM; Sigma-Aldrich) or with concanamycin A (CMA, 100 nM; Sigma-Aldrich) for 30 min.

γδ T cells—iRBC cocultures

Effector cells activated with supernatant of iRBC were incubated with *P. falciparum* late stage (~10% parasitemia) for indicated times and at indicated E:T ratios in MCM. For indicated experiments, a blocking γδ TCR Ab (2 μg/ml, clone 11F2; Miltenyi) was added to the effector cells before the coincubation with the iRBCs.

To visualize the conjugates, the killer cells–iRBCs mixture was washed twice with MCM before fixation with 1.5% paraformaldehyde in PBS. The conjugates were stained with a fluorescently conjugated anti-GzmB Ab (BD Biosciences) using a kit for intracellular marker staining (BD Biosciences), counterstained with Hoechst, mounted in Vectashield, and assessed by confocal microscopy. Some conjugates were stained with a fluorescently conjugated anti-γδTCR Ab (BD Biosciences) or anti-CD3 Ab (Miltenyi).

Treatment of iRBCs with cytotoxic effector molecules

P. falciparum–infected RBCs were washed with PBS and resuspended at 1% HCT in hypotonic cell buffer (40 mM HEPES, pH 7.4, 50 mM NaCl, 4 mM $CaCl_2$, 1% BSA, and 5 mM glucose). iRBCs were treated for 30 min with GzmB in combination with PFN or GNLY (prediluted in hypotonic assay buffer: 40 mM HEPES, pH 7.4, 50 mM NaCl).

Mitochondrial membrane potential

The mitochondrial membrane potential of *P. falciparum*–infected RBCs was demonstrated by the staining of iRBCs with 2 μM JC-1 (Abcam) dye in MCM. Staining was performed for 15 min at 37˚C followed by washes with PBS. Stained iRBCs were coincubated for 1 h with activated γδ T cells in MCM, then stained with Hoechst for assessment by live cell confocal microscopy.

In contrast, iRBCs were treated in hypotonic cell buffer with cytotoxic effector molecules (in assay buffer) for 30 min before being stained with

2 μM JC-1 and 1 μg/ml Hoechst, washed with PBS + 5 mM glucose, and then assessed live by confocal microscopy or flow cytometry.

Reinvasion assays

The killer cells were prestained with 2 μg/ml BCECF-AM for 30 min at 37°C, then washed three times with PBS and coincubated with iRBCs at indicated E:T ratios for 2 h. The cocultures were performed in triplicates in round-bottom 96-well plates with 50,000 killer cells in 100 μl MCM. As controls, the killer cells were additionally pretreated (during the 2,7-Bis(2-carboxyethyl)-5(6)-carboxyfluorescein [BCECF-AM] staining) with DCI (25 μM) or with CMA (100 nM). After the coincubation, the cells were pelleted by centrifugation and diluted by adding 200 μl of non-iRBCs at 1% HCT in complete medium. After 48 h, the cultures were counterstained with 5 μM DRAQ5 (Thermo Fisher Scientific), and parasitemia was measured by flow cytometry.

P. falciparum–infected RBCs in cell buffer, treated with the cytotoxic effector molecules in assay buffer, were pelleted by centrifugation and then diluted by adding 200 μl of non-iRBCs at 1% HCT in complete medium. After 48 h, the cultures were counterstained with 1 μM SYBR green (Thermo Fisher Scientific) and assessed by flow cytometry. Reinvasion was calculated using the following formula: $(\text{parasitemia}_{\text{treated}}/\text{parasitemia}_{\text{controls}})\times 100$.

GzmB uptake

For the assessment of GzmB uptake, GzmB-AF488 was used. After the incubation with effector molecules for 30 min, the cells were washed with PBS, fixed with 1.5% paraformaldehyde, and counterstained with Hoechst before assessing by confocal microscopy.

Dextran uptake

P. falciparum–infected RBCs were treated with low concentrations of PFN (0.25 hu) or GNLY (0.5 μM) for 5 min at room temperature in the presence of dextran 4kD-AF488 (0.1 mM; Sigma-Aldrich) and counterstained with Hoechst. Cells were directly assessed live by confocal microscopy.

Measurement of ATP content

P. falciparum–infected RBCs treated with cytotoxic proteins were mixed 1:1 with the lysis/reaction buffer of the BacTiter-Glo Cell Viability Assay kit (Promega). The mixture was incubated at room temperature for 20 min before the luminescence was measured by plate reader.

Transmission electron microscopy

P. falciparum–infected RBCs treated with cytotoxic proteins were prefixed in 0.1 M cacodylate buffer (2.5% glutaraldehyde and 0.8% paraformaldehyde), postfixed with an aqueous solution (1% OsO_4 and 1.5% $K_4Fe[CN]_6$), and embedded into epon. Ultrathin sections (50 nm) were contrasted with lead citrate and uranyl acetate and analyzed with a CM 100 (Philips).

Assessment of plasmodial substrate cleavage

Escherichia coli Bl21 harboring GST-fusion protein in pGEX4Ti were induced for 60 min at 37°C with 0.25 mM isopropyl β-D-1-thiogalactopyranoside (IPTG) in Luria-Bertani broth containing 100 μg/ml ampicillin and 2% glucose, washed, and resuspended in 20 mM NaCl, 10 mM Tris (pH 7.4) before adding Gzms and sublytic GNLY, as described (18). Reactions were stopped by boiling in SDS-PAGE loading buffer. Samples were analyzed by immunoblot using anti-GST mAb (BD Biosciences).

Flow cytometry

Cells were analyzed using multicolor flow cytometer: MACSQuant (Miltenyi) or Accuri C6 (BD Biosciences). Data were analyzed using FlowJo software (Ashland, OR)

Confocal laser scanning microscopy

Fluorescent-labeled specimens were examined using a confocal laser scanning microscope (SP5; Leica). Image acquisition was performed with 40× and 63× objectives. Images were analyzed with Imaris 9.1 software (Bitplane AG, Zürich, Switzerland) applying background subtraction and threshold application.

Statistics

Data are presented as means ± SEM. Comparisons between the different groups were performed with two-tailed unpaired Student *t* tests. The *p* values are indicated in the figures, and *p* values of <0.05 were considered significant.

Results

γδ T cells expand and develop cytolytic potential in response to P. falciparum*–infected RBC supernatants*

In humans in vivo (10, 29) and under in vitro (26) conditions using PBMCs, *P. falciparum* infection increases the percentage and absolute number of γδ T cells. When we treated PBMCs with culture supernatant of *P. falciparum*–infected RBCs and IL-2, we found an expansion of γδ T cells from <2% to >50% after 14 d of coincubation, whereas αβ T cells were less affected. Importantly, to exclude donor-specific variations, all the experiments in this study used PBMCs of at least four donors. In control cultures, activated with the supernatant of non-iRBCs + IL-2 or with IL-2 alone, γδ T cells were far less expanded (Fig. 1A, 1B). CFSE staining for flow cytometry demonstrated that >90% of the γδ T cells proliferated upon stimulation with iRBC supernatant and IL-2 (Supplemental Fig. 1A). Consistent with previous work (26), size fractionation of the iRBC supernatant revealed a small molecule of <10 kDa responsible for the activation of γδ T cells (Supplemental Fig. 1B), most likely a soluble phosphoantigen. Confocal microscopy showed that the cells, activated with iRBC supernatant and IL-2, grow in big clusters, most of which highly expressed the γδ TCR, and only a few displayed surface CD56 staining, normally increased in IL-2–activated PBMC cultures (30) (Fig. 1C, 1D). Strikingly, most of these clustered cells highly expressed the major cytotoxic effector proteins, in particular GzmB (Fig. 1E) but also GNLY and PFN (Fig. 1F), and displayed Gzm- and PFN-dependent cytolytic activity against the cell line K562 (Fig. 1G). A hallmark of γδ T cells in human malaria is the early production of IFN-γ (31). PBMCs, which were activated with iRBC supernatant and IL-2, produced significantly higher amounts of IFN-γ in the second week of activation as compared with control PBMCs activated with noninfected supernatant or with IL-2 alone (Fig. 1H). In addition, intracellular cytokine staining in flow cytometry revealed the major source of IFN-γ to be γδ T cells upon activation with iRBC supernatant and IL-2 (Fig. 1I).

γδ T cells bind P. falciparum*–infected RBCs to transfer GzmB*

To test the possible role of γδ T cells as killer cells against *P. falciparum*–infected RBCs, we incubated the activated effector population with *P. falciparum*–infected RBCs and stained for T cell surface markers and GzmB. Abs against the pan-γδ TCR and CD3 surface staining indicated that γδ T cells formed conjugates with iRBCs (Fig. 2A). Early and late parasite stages were found conjugated to these effector cells. Allele-specific staining demonstrated the presence of the Vδ2 chain at the surface of the conjugated effector cells (Fig. 2B). Double staining of the conjugates with Abs against the δ2 chain and intracellular GzmB indicated polarization of the cytolytic granules in the γVδ2 T cells toward the immunological synapse (Fig. 2C), typically observed in immune conjugates between effector and target cells (32). High-resolution confocal microscopy clearly revealed that within many of these conjugates GzmB was transferred into the bound iRBCs to be found in close proximity to parasite DNA (Fig. 2D). To estimate the frequency of conjugate formation between killer cells and iRBCs, we analyzed in lower-magnification images the formation of conjugates between iRBCs and killer cells that were stained for GzmB to judge cell polarization. Although this assessment was complicated by the tendency of iRBCs to form bigger clusters (33, 34) (Fig. 2E) as compared with non-iRBCs (Fig. 2F), we found that ~8% of the iRBCs were bound to killer cells (Fig. 2G).

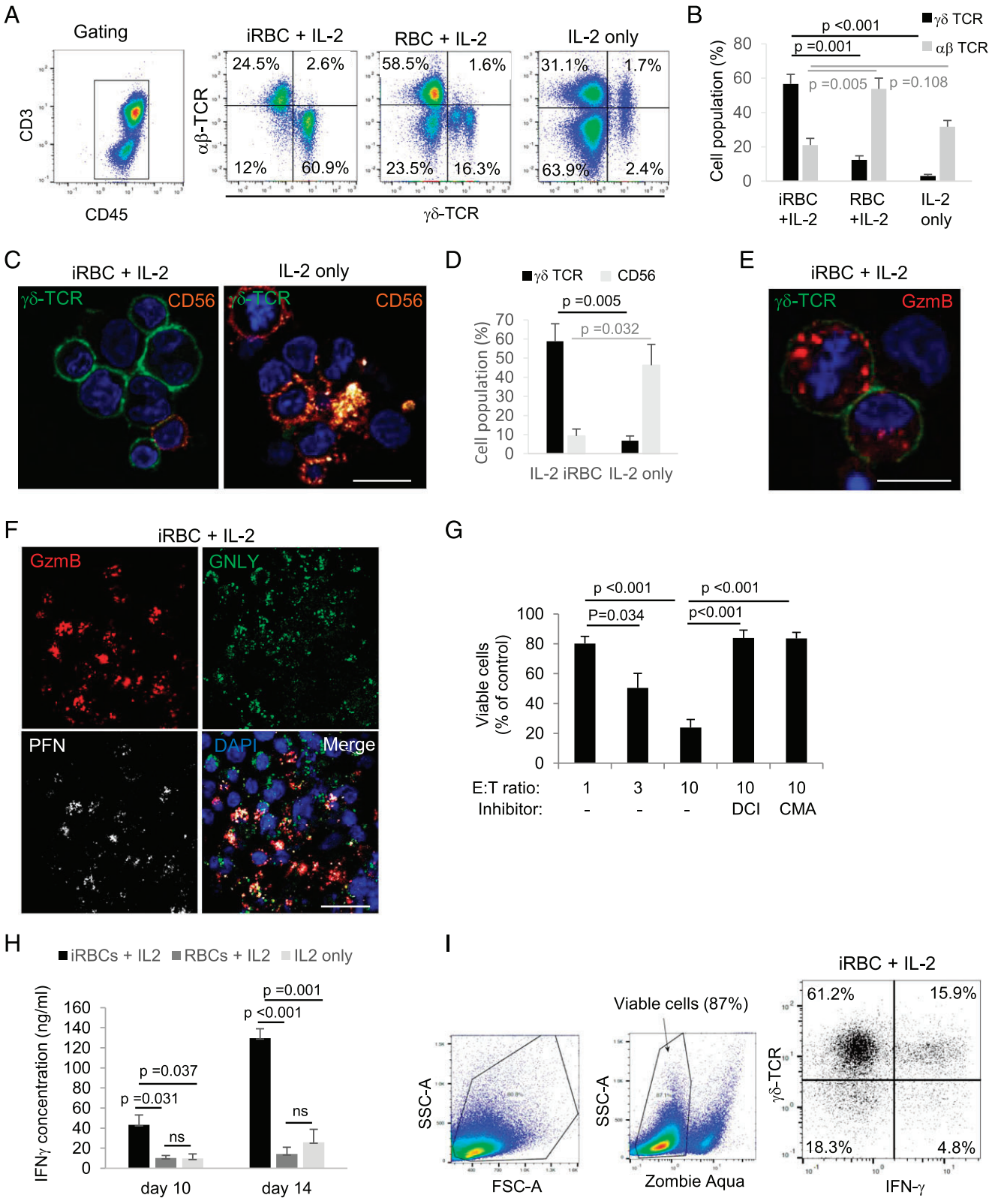

FIGURE 1. γδ T cells expand and develop cytolytic potential in response to *P. falciparum*–infected RBC supernatants. PBMCs were treated with culture supernatant of parasitized RBCs (iRBCs) and IL-2, with supernatant of non-iRBCs + IL-2, or with IL-2 alone for 14 d. Following the activation, the cells were stained with anti-CD3/anti-CD45 Abs (**A** for the gating), TCR Abs (A, **C**, and **E**), Abs against CD56 (C), and Abs against cytotoxic effector molecules (E and **F**) for analysis by flow cytometry and confocal microscopy. For microscopy, the nuclei were stained with DAPI. Scale bars, 10 μm (C and E) and 20 μm (F). (**B**) The quantification of three independent flow cytometry experiments (using PBMCs of two different donors) concerning the frequency of γδ versus αβ TCR expression. The microscopy results of (C) were quantified by counting 50 cells per condition in three independent experiments as shown in (**D**). (**G**) iRBC-activated cells were analyzed for their cytolytic potential in fluorescence release assays against the target cell line K562 at indicated E:T ratios. DCI was used to inhibit Gzm activity, and CMA served as a PFN inhibitor. (**H**) IFN-γ levels in the supernatants of cultures with indicated activation conditions were measured by ELISA. (**I**) A representative cytometry plot of three independent experiments demonstrating intracellular IFN-γ in γδ T cells. (B, D, G, and H) Bars represent average ±SEM in three independent experiments. The *p* values of statistical differences between groups, calculated by Student *t* test, are indicated.

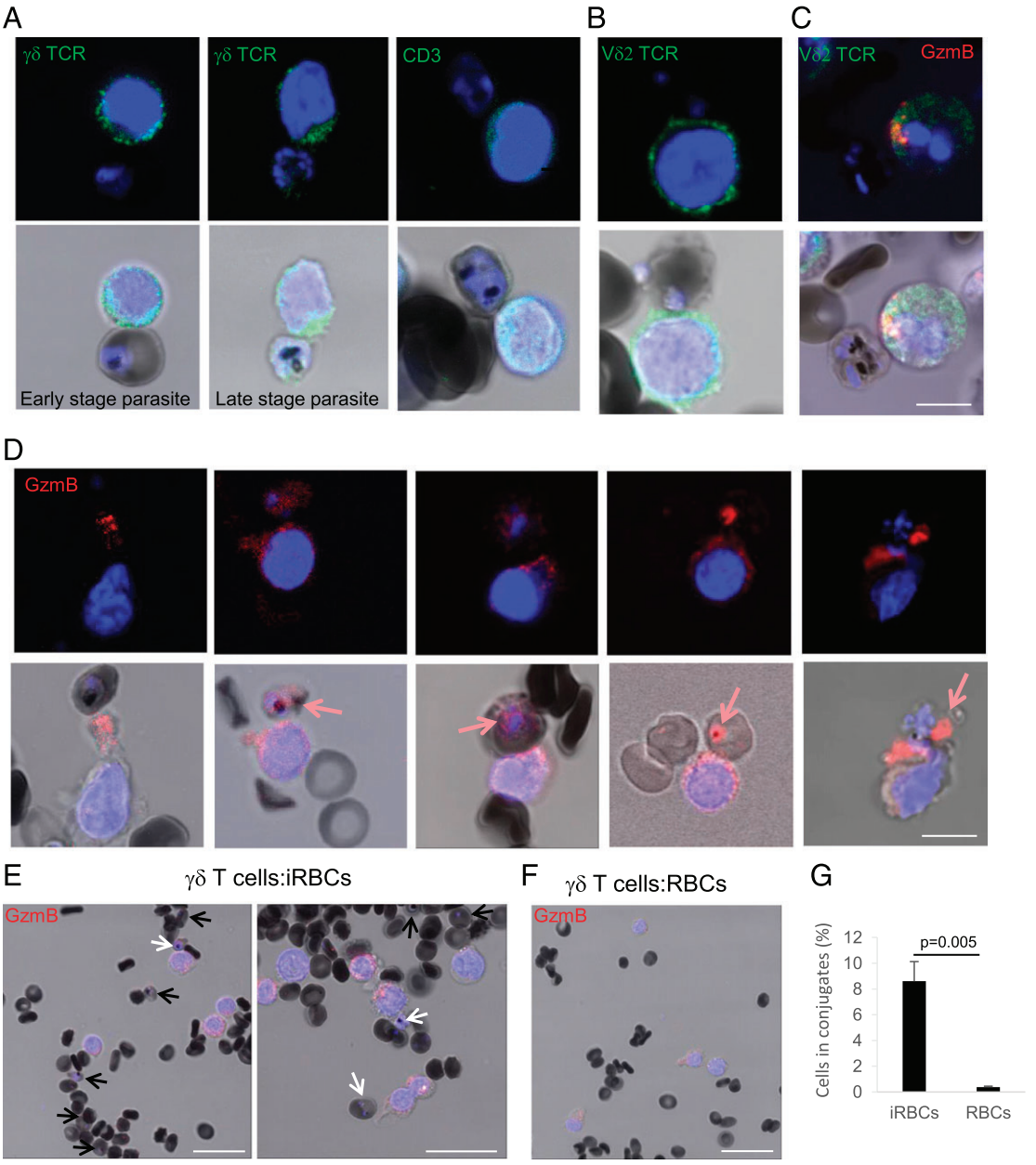

FIGURE 2. γδ T cells bind *P. falciparum*–infected RBCs to release GzmB. Effector cells activated with iRBC supernatant and IL-2 were incubated with *P. falciparum*–infected RBCs for 60 min and stained with indicated T cell surface markers (green in **A**–**C**), GzmB Ab (red in C–**F**), and Hoechst as nuclear marker (blue). Formation of stable conjugates between killer cells and iRBCs was visualized by confocal microscopy. Scale bars, 10 μm (A–D) and 20 μm (E and F). Representative images of at least four independent experiments are presented. (D) Transfer of GzmB into iRBCs is indicated with red arrows in the merge images. (E) iRBCs in conjugation with killer cells are indicated with white arrows, and unconjugated iRBCs are indicated with black arrows. (**G**) Quantification of the frequency of RBC–killer cell conjugations. One hundred iRBCs and >200 RBCs were counted in three independent experiments.

γδ T cells reduce P. falciparum *viability in iRBCs and the reinvasion capacity of the parasites in a Gzm-dependent manner and independently of PFN*

In addition to the transfer of GzmB into iRBCs, killer cell–infected RBC conjugate formation reduced the viability of the parasite as indicated at the single-cell level by the decrease of signal intensity of the mitochondrial potential indicator JC-1 (35) (Fig. 3A). To assess the impact of the supernatant-activated killer cells on parasite viability at the population level, we performed reinvasion assays using synchronized late-stage parasite cultures coincubated with BCECF-labeled killer cells. The parasitemia in the cultures was measured after 48 h using the DNA stain DRAQ5 in flow cytometry. Indeed, the coincubation of iRBCs with activated cells significantly reduced parasitemia, indicating reduced reinvasion capacity of the parasites in response to the killer cell attack (Fig. 3B, 3C). Pretreatment of the killer cells with the serine protease inhibitor DCI, known to disable Gzm activity (36), completely abrogated their ability to block reinvasion, confirming the need for Gzm to kill parasites. In contrast to the killing of K562 cells (Fig. 1G), pretreatment with CMA, a known inhibitor of PFN (37), did not significantly alter the ability of the killer cells to inhibit reinvasion. MACS of the activated cells indeed revealed γδ T cells (enriched MACS in Fig. 3D) as the major lytic population, whereas the flow-through cells (non–γδ T cells = depleted MACS in Fig. 3D) were significantly less inhibitory toward the parasite reinvasion (Fig. 3E). However, there was a significant reduction of reinvasion compared with no effector cell controls also in response to the non–γδ T cells, probably because of the

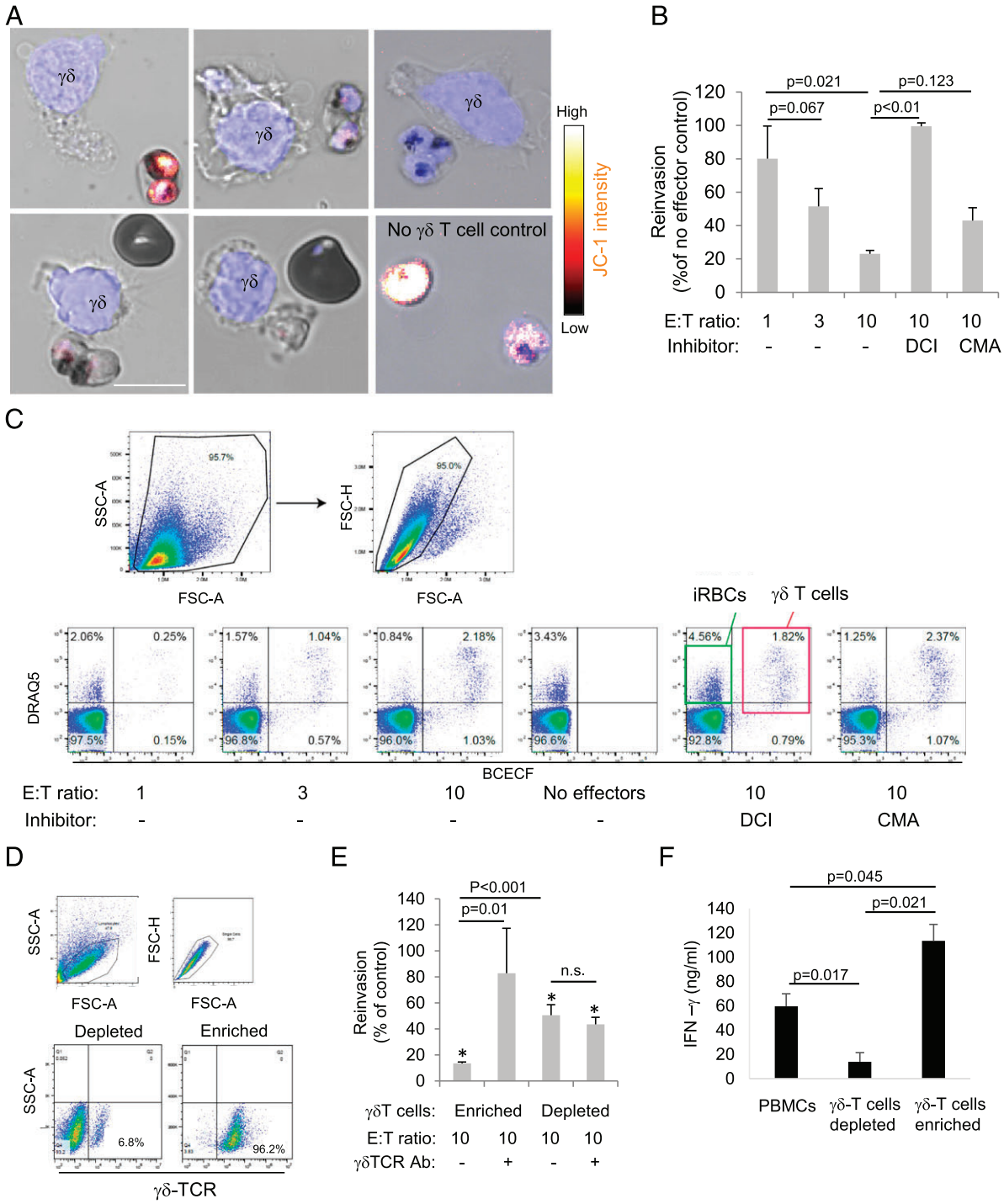

FIGURE 3. γδ T cells reduce *P. falciparum* viability in iRBCs and the reinvasion capacity of the parasites. (**A**) Activated γδ T cells were incubated with JC-1–prestained late-stage iRBCs for 30 min and then stained with Hoechst as nuclear marker (blue) before JC-1 staining intensity was assessed by life cell microscopy. Scale bar, 10 μm. (**B**) Activated γδ T cells, prelabeled with BCECF-AM, were incubated with late-stage iRBCs for 2 h at indicated E:T ratios before dilution in uninfected RBCs to assess reinvasion capacity. After 48 h, the cultures were stained with DRAQ5, and parasitemia was measured by flow cytometry. DCI and CMA were used to inhibit Gzm and PFN activity, respectively. (**C**) The gating strategy of a representative experiment is presented. (**D**) We show a representative flow cytometry analysis using γδ TCR Abs of cells that were MACS purified (enriched for or depleted of γδ T cells) and further activated with iRBC supernatant and IL-2 for 6 d. (**E**) These purified cells (γδ-enriched versus γδ-depleted PBMCs) were tested in reinvasion assays as above, including the addition of a blocking γδ TCR Ab to the effector cells just before the coincubation with iRBCs. In addition, the supernatant of enriched γδ T cells compared with γδ T cell–depleted cultures or unpurified PBMCs after 10 d of activation with iRBC supernatant and IL-2 were tested for INF-γ levels by ELISA. Averages ±SEM of the normalized reinvasion capacity of four independent experiments are shown (B, E, and **F**). The *p* values of differences between groups, calculated by Student *t* test, are indicated. (E) The asterisks (*) represent statistical differences (Student *t* test) to no-effector cell controls.

IL-2–activated NK cells ($CD56^+$ LAK cells) in these cultures (38). Importantly, the addition of a γδ TCR–blocking Ab to the cocultures significantly impaired the inhibitory activity of the enriched γδ T cells, but not of enriched γδ T cell depleted population, suggesting involvement of the γδ TCR in the killing mechanism (Fig. 3E). In addition, the enriched γδ T cells proved to be the

major source of IFN-γ production upon stimulation with iRBC supernatant as compared with unsorted PBMCs or the enriched γδ T cell depleted fraction (Fig. 3F; also compare Fig. 1I).

GNLY delivers GzmB into late-stage P. falciparum*–infected RBCs and merozoites*

To dissect the molecular events of GzmB-mediated killing of the parasite during the blood stage, we tracked the delivery of fluorescently labeled GzmB into RBCs (Fig. 4A, Supplemental Fig. 2). Interestingly, GNLY specifically delivered GzmB into late-stage iRBCs, whereas uninfected and early-stage iRBCs remained unaffected (Fig. 4B). GzmB was unspecifically delivered by PFN in noninfected cells and in all stages of iRBCs. However, the delivery into late stages was significantly less efficient as by GNLY (Fig. 4B), suggesting a decreased susceptibility of late-stage iRBC membranes toward PFN lysis. In line with a recent study demonstrating merozoites susceptible to GNLY lysis (17), we also found delivery of GzmB into merozoites by GNLY (Fig. 4C), although we could not quantify these events because free merozoites were only rarely detected in the mixed cultures. To further investigate the stage-specific susceptibility of iRBCs, we assessed the influx of fluorescently labeled 4-kDa dextran in response to GNLY and PFN treatment (39). In this experimental setup, the specificity of these two cytolytic proteins was contrary. Whereas during PFN treatment, multinucleated late stages excluded the dye, early-stage iRBCs and uninfected RBCs rapidly filled up with the labeled dextran. In contrast, GNLY treatment delivered dextran exclusively into late stages but not in early-stage iRBCs or uninfected cells (Fig. 4D, 4E).

GNLY-delivered GzmB reduces ATP production as well as reinvasion capacity of late-stage parasites and cleaves essential plasmodial proteins

To understand the consequences of GNLY-delivered GzmB, we measured the ATP production in synchronized parasite cultures at both early (rings) and late stages (trophozoites and schizonts). Indeed, GNLY specifically delivered GzmB into late-stage parasites, indicated by the significant reduction in ATP production (Fig. 5A), whereas rings were not affected (Fig. 5B). As already observed by confocal microscopy (Fig. 4A), PFN delivered GzmB into all stages of iRBCs, therefore equally affecting the ATP content of early- and late-stage parasites. This effect seemed to be mostly driven by PFN-induced hemolysis as the cotreatment with GzmB did not significantly further decrease the ATP content in the parasites (Fig. 5A, 5B). In line with these data, we found in reinvasion assays that GzmB dose dependently inhibited the reinvasion capacity of synchronized late-stage parasites when delivered by GNLY. Again, PFN treatment alone inhibited reinvasion that was not significantly further enhanced by the cotreatment with GzmB (Fig. 5C).

A crucial line of evidence for the claim that γδ T cells restrict parasite growth in a Gzm-dependent manner is the identification of plasmodial proteins that are targeted and efficiently destroyed by the effector immune proteases. Recent studies revealed that oxidative defense enzymes (18, 19), the Clp protease system, and the virulence machinery (40) are predominantly targeted in microbial pathogens by the Gzms. In this study, we found that ClpR, a proteolytic subunit of the Clp system in *P. falciparum*, the major antioxidant enzyme 1-cys peroxiredoxin (1-cys Pxn), as well as the extracellular domain of one of the rifins, essential plasmodial virulence mediators, were efficiently cleaved by GzmB. However, superoxide dismutase B (SodB), which is cleaved in *Trypanosoma* and several bacterial pathogens, is not targeted in *P. falciparum* (Fig. 5D).

GzmB damages the mitochondrial membrane potential and induces drastic morphological alterations in late-stage parasites when delivered by GNLY

To further investigate the cytolytic mechanism that is mediated by GNLY-delivered GzmB in late-stage parasites, we treated late iRBCs with GzmB ± GNLY and assessed the viability of parasites with JC-1. The combined treatment with GNLY and GzmB markedly reduced the JC-1 staining intensity at the single-cell level (Fig. 6A). These microscopic results were confirmed using flow cytometry in which we not only found a drop in parasitemia but also a significant reduction of JC-1 staining intensity when the iRBCs were cotreated with the effector molecules (Fig. 6B, 6C). Strikingly, we also observed drastic ultrastructural morphological alteration in transmission electron microscopy (Fig. 6D). Although GNLY only–treated late-stage parasites were undistinguishable from untreated iRBCs, the combined treatment with GNLY and GzmB affected the host cells (loss of hemoglobin), the parasitophorous vacuole membrane, and the intracellular parasites with an almost complete loss of organelle features, such as the nucleus and the apical organelles (41). These results indicate that GNLY in these low nanomolar concentrations is per se nonlytic to the iRBCs, and only the combination with GzmB leads to this rapid loss of plasmodial mitochondrial membrane potential and committing loss of ultrastructural integrity.

Discussion

γδ T cells, in particular the cellular subset bearing the Vγ9Vδ2 TCR (12), were suspected for decades to play a significant role in protective immunity against the malaria parasite, especially in naive hosts during a primary infection (42, 43). However, the mechanism of how they convey this protection was less clear. During a primary malaria infection, γδ T cells expand drastically in the peripheral blood and spleens of humans and mice (10, 11, 44–46). γδ T cells proliferate in vitro in a TCR-dependent manner in response to soluble mediators, in particular phosphoantigens, that are released during the schizont burst (26). For this proliferative response, cell-to-cell contact is not required. In line with these data, we found a massive expansion of γδ T cells in vitro when PBMCs were treated with cell-free iRBCs supernatants, and in addition, we could confirm that the activating compound in the supernatant has a molecular size of $<$10 kDa. As an important addition to the proliferative response, we found that these expanded γδ T cells developed high cytolytic potential and produce vast amounts of IFN-γ.

In contrast to the proliferative response, contact (or close proximity) between γδ T cells and the iRBCs is required for inhibition to occur (16, 47, 48). In line with our data, Costa et al. (17) recently provided strong evidence that γVδ2 T cells inhibit parasite expansion during the blood stage in a contact- and GNLY-dependent manner. However, when the authors removed the killer cells from the cocultures with purified trophozoites by MACS after 6 h, the inhibitory activity was lost. From this experiment, they concluded that γδ T cells mainly act on merozoites. In the same study, it was also demonstrated that schizont-stage iRBCs induced the same level of γδ T cell degranulation (CD107 positivity) in a TCR-dependent manner than cocultures with merozoites. Therefore, we consider this conflicting result as a consequence of the timing of the cocultures. γδ T cells might have to be present at the late trophozoites and schizont stage to mediate the inhibition. In addition, this particular study used a different parasite strain (FCR3), which might also contribute to the varying outcome.

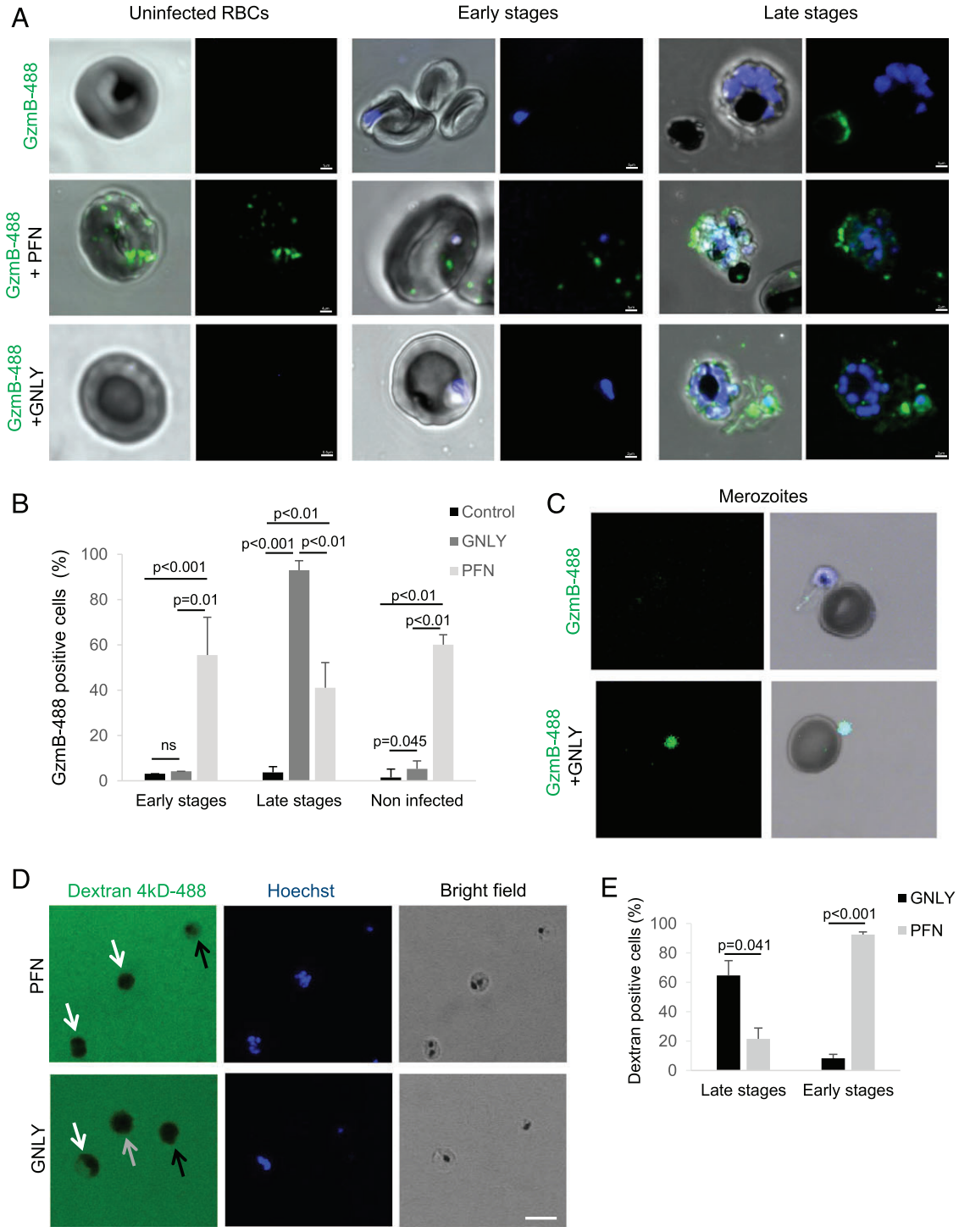

FIGURE 4. Transfer of GzmB is mediated by GNLY in a stage-specific manner. Uninfected and nonsynchronized iRBC cultures were treated with Alexa Fluor 488–labeled GzmB (0.4 μM) in combination with PFN (0.25 hu) or GNLY (0.5 μM) for 20 min before fixation and assessment by confocal microscopy. Intraerythrocytic forms (early and late stages) are shown in (**A**) and Supplemental Fig. 1, and merozoites are presented in (**C**). Nuclei were stained with Hoechst. Scale bars, 2 μm in (A) and 5 μm in (C). (**B**) Over 100 cells per condition in four independent experiments were assessed for intracellular GzmB and quantified. Averages ±SEM of GzmB-488–containing cells in three independent experiments are shown. The *p* values of differences between groups, calculated by Student *t* test, are indicated. Representative visual fields used for the quantification are shown in Supplemental Fig. 1. (**D**) Unsynchronized iRBCs of high parasitemia were treated with PFN or GNLY for 5 min in presence of fluorescently labeled dextran and Hoechst and then assessed live by confocal microscopy. Late stages are indicated with white arrows, early stages are indicated with black arrows, and uninfected RBCs are indicated with a gray arrow. Scale bar, 10 μm. (**E**) Dextran uptake in late- and early-stage iRBCs upon GNLY or PFN treatment was quantified by counting 30 cells per condition in three independent experiments.

In this study, we provide additional evidence that γδ T cells, particularly γVδ2 T cells, bind *P. falciparum*–infected RBCs to form immune conjugates. We also demonstrate that the killer cells release GzmB, which is transferred into the bound iRBCs. More importantly, we show that the parasite viability was rapidly reduced within these conjugates. Activated killer cells depleted of

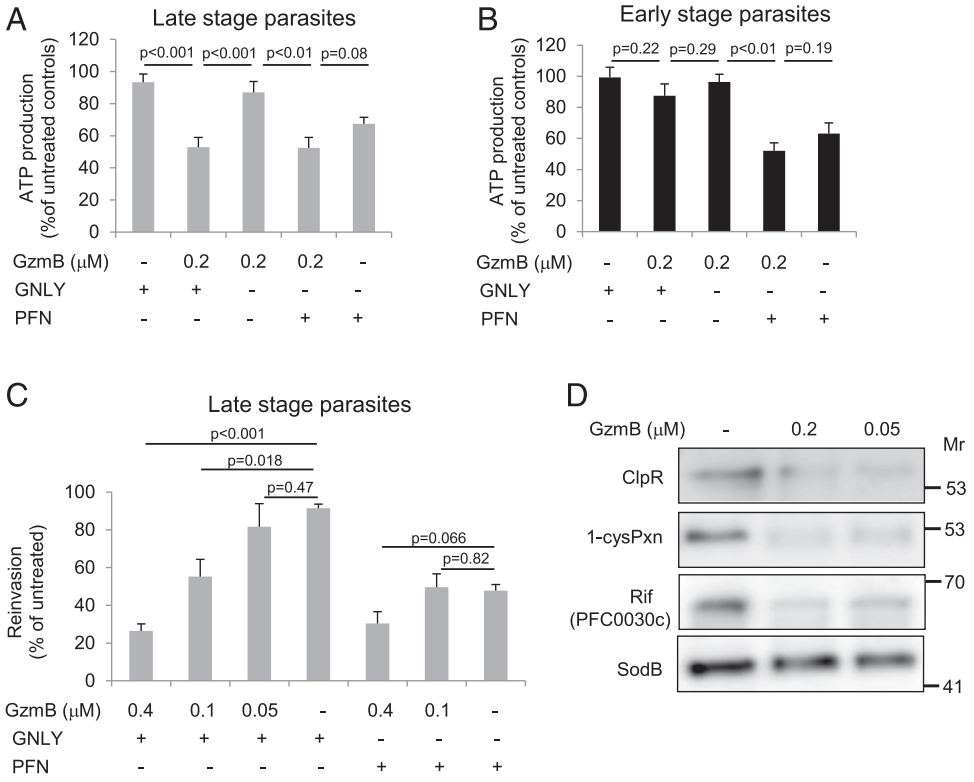

FIGURE 5. GzmB inhibits ATP production as well as the reinvasion capacity of late-stage parasites and cleaves essential plasmodial proteins. Synchronized early- and late-stage iRBCs were treated with GzmB at indicated concentrations in combination with GNLY (0.5 μM) or PFN (0.25 hu) for 60 min before assessment of ATP production (**A** and **B**) and reinvasion capacity after 48 h (**C**). Averages ±SEM of at least four independent experiments are presented. (**D**) *E. coli* expressing GST-tagged ClpR, 1-cysPxn, Rif (PFC0030c), or SodB were treated with indicated doses of GzmB + sublytic GNLY for 30 min before substrate cleavage was assessed in anti-GST immunoblots.

γδ T cells by MACS were significantly less efficient to reduce parasite viability and secrete IFN-γ and, therefore, impact reinvasion. We present evidence that suggests involvement of the γδ TCR in the inhibitory mechanism as a blocking Ab significantly reduced inhibitory activity of this effector cell population. What ligand the γδ TCR recognizes on the iRBCs is up to speculation. For the γδ TCR–mediated recognition of microbial infected nucleated cells, a crucial role of CD277 (butyrophilin 3A1, BNT3A1), a type I glycoprotein in the B7 family, was recently demonstrated (49). Importantly, activation of γδ T cells by plasmodial derived phosphoantigens depends on the presence of the TCR and BTN3A (26). However, as BNT3A1 was not identified on iRBCs (26), a major role in the context of blood-stage malaria is called into question. Other ligands, such as the F1-ATPase (50) or the endothelial protein C receptor (51), were implicated in the recognition of stressed cells, and their potential roles in blood-stage malaria have yet to be elucidated. Furthermore, we show that the lytic effect was dependent on Gzm activity as the serine protease inhibitor, DCI, abolished the impact of γδ T cells on the reinvasion capacity of the parasites. The inhibitory activity of γδ T cells was, in contrast, independent of PFN activity, as the known PFN inhibitor, CMA (37), had no effect on the reinvasion capacity. This is in line with the above-discussed Costa et al. (17) study demonstrating that the inhibitory activity of γδ T cells against blood-stage parasites was independent on PFN activity.

An intriguing question remains of how γδ T cell cytotoxicity may contribute to antimalaria immune defense under physiological in vivo conditions. Although the frequency of γδ T cells in the peripheral blood increases drastically during a primary malaria infection for about 4 wk (10), and these cells also upregulate their cytotoxic granule proteins (17, 52), it is not likely that iRBCs encounter and bind activated γδ T cells in the blood stream at an E:T ratio of 10 as in this current in vitro study. However, it is well established that late trophozoites and schizonts sequester in the microvasculature, creating a proinflammatory environment (53) that may lead to the recruitment of effector cells, such as activated γδ T cells. It was demonstrated in mice that γδ T cells migrate to these inflammatory sites and their overreactivity critically contribute to a local immune pathologic condition, such as cerebral malaria (54, 55). At these sites in various tissues, direct contact and conjugate formation between killer cells and γδ T cells might be favored. Also, the red pulp of the spleen might represent a preferred site for these encounters, in particular the slow open microcirculation (56), where γδ T cells are preferentially localized (44). In line with that is the observation that splenomegaly is a common clinical feature in *P. falciparum* endemic areas (57).

On the molecular level, we show that the mammalian membrane pore-forming protein PFN promoted transfer of GzmB in all stages of iRBCs and non-iRBCs, whereas GNLY triggered uptake of GzmB exclusively into late-stage iRBCs and merozoites independently of PFN. GNLY is a prokaryotic membrane-disrupting effector molecule that under regular conditions does not impair the plasma membrane integrity of cholesterol-rich mammalian cells (58). What renders late-stage iRBCs susceptible to GNLY remains to be investigated. Interestingly, the parasite alters the membrane lipid composition of the host cells in the course of the infection (59), potentially making them more vulnerable to GNLY-mediated lysis. It has been shown that the trophozoite development depletes the RBC plasma membrane of cholesterol (60). We hypothesize that this cholesterol depletion renders late-stage iRBCs more susceptible to GNLY (58). Our cotreatment experiments with labeled dextran additionally suggested that cholesterol-depleted late-stage iRBC membranes became more resistant to PFN lysis.

Importantly, GzmB drastically reduces the parasite viability when delivered into the iRBCs by membrane-disrupting proteins, in particular by GNLY into late-stage iRBCs. The biological significance of this observation is supported by several published lines of evidence: 1) a GzmB single-chain Ab fusion construct directed against merozoites inhibited parasite growth (61), 2) γδ T cells exhibited antimalarial activity in a GNLY-dependent mechanism (16, 17), 3) innate immune killer cells upregulate and release GzmB in response to iRBCs (52), and 4) Gzms (62) as

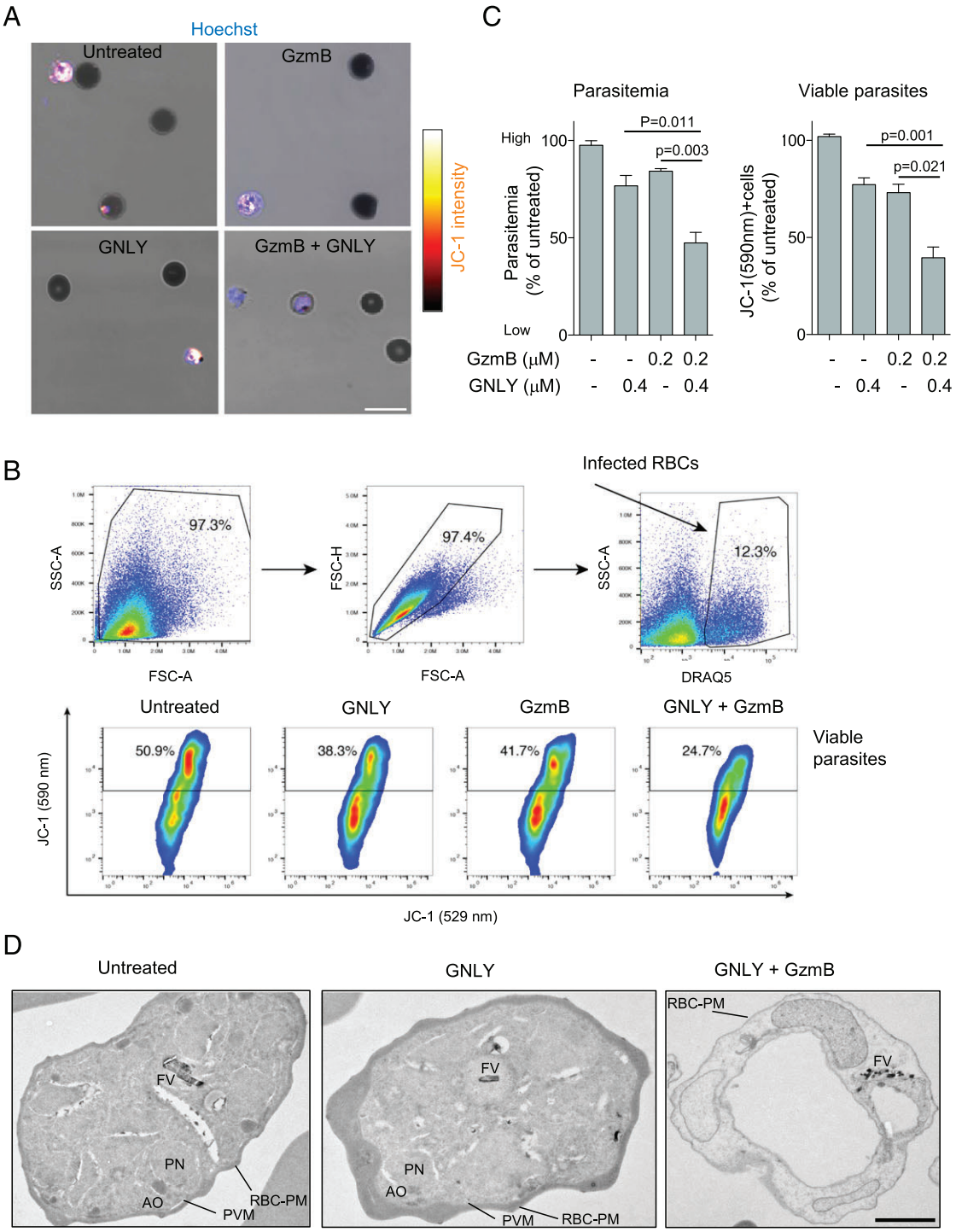

FIGURE 6. GzmB triggers loss of mitochondrial membrane potential and induces drastic morphological alterations in late-stage parasites when delivered by GNLY. iRBCs were treated with GzmB ±GNLY for 30 min and were then stained with the MitoProbe JC-1 before assessment by confocal microscopy (**A**) and flow cytometry (**B** and **C**). For microscopy, parasites were stained with Hoechst, and for flow cytometry, iRBCs were labeled with DRAQ5. Representative images are presented in (A), and the gating strategy of a representative flow cytometry experiment is shown in (B). Averages ±SEM of normalized parasitemia and JC-1 red staining percentage (viable parasites) of four independent experiments are shown in (C). (**D**) iRBCs were treated with GNLY (0.5 μM) ±GzmB (0.2 μM) for 60 min and then processed for analysis by transmission electron microscopy. Scale bar, 1 μm. Identifiable structures are indicated: RBC plasma membrane (RBC-PM) with knob structures, parasitophorous vacuole membrane (PVM), parasite nucleus (PN), apical organelles (AO), and food vacuole (FV).

well as GNLY levels (17) are elevated in *P. falciparum*–infected individuals. Additionally, it was recently demonstrated that $CD8^+$ T cells expand and upregulate GzmB as well as PFN during *Plasmodium vivax* infections in the human blood (63) and, potentially, lyse the parasites in reticulocytes in a Gzm-dependent manner (64). In this study, we revealed that incubation with GzmB in combination with PFN reduces the viability of both early stages and late stages of the parasite. However, this reduction of viability seems to be mostly driven by the iRBC lysis mediated by PFN as we could not detect a significant additional inhibition when the iRBCs were treated with PFN and GzmB compared with PFN treatment alone. More importantly, the combination of GzmB and

GNLY decreased the viability and ultrastructural integrity in late stages of the parasite, whereas early stages were not affected by this treatment combination, most probably because GNLY treatment does not allow the entry of GzmB into these iRBC stages.

Our discovery of protein substrates within the plasmodial proteome that were efficiently destroyed by GzmB strongly supports our hypothesis that the delivery of proteolytically active GzmB into the parasite is the driving force for the observed decrease of parasite viability.

Overall, our data establish a novel (to our knowledge) innate immune mechanism of how γδ T cells provide immune protection against blood-stage malaria by the specific binding to iRBCs to release the cytotoxic effector molecules GzmB and GNLY that subsequently efficiently kill the intracellular late-stage parasites.

Disclosures

The authors have no financial conflicts of interest.

References

1. WHO. 2017. World Malaria Report 2017. Available at: https://www.who.int/malaria/publications/world-malaria-report-2017/en/.
2. Miller, L. H., H. C. Ackerman, X. Z. Su, and T. E. Wellems. 2013. Malaria biology and disease pathogenesis: insights for new treatments. *Nat. Med.* 19: 156–167.
3. Murugan, R., L. Buchauer, G. Triller, C. Kreschel, G. Costa, G. Pidelaserra Martí, K. Imkeller, C. E. Busse, S. Chakravarty, B. K. L. Sim, et al. 2018. Clonal selection drives protective memory B cell responses in controlled human malaria infection. *Sci. Immunol.* 3: eaap8029.
4. Beeson, J. G., F. H. Osier, and C. R. Engwerda. 2008. Recent insights into humoral and cellular immune responses against malaria. *Trends Parasitol.* 24: 578–584.
5. Lönnberg, T., V. Svensson, K. R. James, D. Fernandez-Ruiz, I. Sebina, R. Montandon, M. S. Soon, L. G. Fogg, A. S. Nair, U. Liligeto, et al. 2017. Single-cell RNA-seq and computational analysis using temporal mixture modelling resolves Th1/Tfh fate bifurcation in malaria. [Published erratum appears in 2018 *Sci. Immunol*. 3: eaat1469.] *Sci. Immunol.* 2: eaal2192.
6. Sabchareon, A., T. Burnouf, D. Ouattara, P. Attanath, H. Bouharoun-Tayoun, P. Chantavanich, C. Foucault, T. Chongsuphajaisiddhi, and P. Druilhe. 1991. Parasitologic and clinical human response to immunoglobulin administration in falciparum malaria. *Am. J. Trop. Med. Hyg.* 45: 297–308.
7. Teo, A., G. Feng, G. V. Brown, J. G. Beeson, and S. J. Rogerson. 2016. Functional antibodies and protection against blood-stage malaria. *Trends Parasitol.* 32: 887–898.
8. Nielsen, M. M., D. A. Witherden, and W. L. Havran. 2017. γδ T cells in homeostasis and host defence of epithelial barrier tissues. *Nat. Rev. Immunol.* 17: 733–745.
9. Deroost, K., and J. Langhorne. 2018. Gamma/Delta T cells and their role in protection against malaria. *Front. Immunol.* 9: 2973.
10. Ho, M., P. Tongtawe, J. Kriangkum, T. Wimonwattrawatee, K. Pattanapanyasat, L. Bryant, J. Shafiq, P. Suntharsamai, S. Looareesuwan, H. K. Webster, and J. F. Elliott. 1994. Polyclonal expansion of peripheral gamma delta T cells in human *Plasmodium falciparum* malaria. *Infect. Immun.* 62: 855–862.
11. Roussilhon, C., M. Agrapart, J. J. Ballet, and A. Bensussan. 1990. T lymphocytes bearing the gamma delta T cell receptor in patients with acute *Plasmodium falciparum* malaria. *J. Infect. Dis.* 162: 283–285.
12. Dantzler, K. W., and P. Jagannathan. 2018. γδ T cells in antimalarial immunity: new insights into their diverse functions in protection and tolerance. *Front. Immunol.* 9: 2445.
13. Russell, J. H., and T. J. Ley. 2002. Lymphocyte-mediated cytotoxicity. *Annu. Rev. Immunol.* 20: 323–370.
14. Walch, M., E. Eppler, C. Dumrese, H. Barman, P. Groscurth, and U. Ziegler. 2005. Uptake of granulysin via lipid rafts leads to lysis of intracellular *Listeria* innocua. *J. Immunol.* 174: 4220–4227.
15. Stenger, S., D. A. Hanson, R. Teitelbaum, P. Dewan, K. R. Niazi, C. J. Froelich, T. Ganz, S. Thoma-Uszynski, A. Melián, C. Bogdan, et al. 1998. An antimicrobial activity of cytolytic T cells mediated by granulysin. *Science* 282: 121–125.
16. Farouk, S. E., L. Mincheva-Nilsson, A. M. Krensky, F. Dieli, and M. Troye-Blomberg. 2004. Gamma delta T cells inhibit in vitro growth of the asexual blood stages of *Plasmodium falciparum* by a granule exocytosis-dependent cytotoxic pathway that requires granulysin. *Eur. J. Immunol.* 34: 2248–2256.
17. Costa, G., S. Loizon, M. Guenot, I. Mocan, F. Halary, G. de Saint-Basile, V. Pitard, J. Déchanet-Merville, J. F. Moreau, M. Troye-Blomberg, et al. 2011. Control of Plasmodium falciparum erythrocytic cycle: γδ T cells target the red blood cell-invasive merozoites. *Blood* 118: 6952–6962.
18. Walch, M., F. Dotiwala, S. Mulik, J. Thiery, T. Kirchhausen, C. Clayberger, A. M. Krensky, D. Martinvalet, and J. Lieberman. 2014. Cytotoxic cells kill intracellular bacteria through granulysin-mediated delivery of granzymes. [Published erratum appears in 2015 *Cell*. 161: 1229.] *Cell* 157: 1309–1323.
19. Dotiwala, F., S. Mulik, R. B. Polidoro, J. A. Ansara, B. A. Burleigh, M. Walch, R. T. Gazzinelli, and J. Lieberman. 2016. Killer lymphocytes use granulysin, perforin and granzymes to kill intracellular parasites. *Nat. Med.* 22: 210–216.
20. Trager, W., and J. B. Jensen. 1976. Human malaria parasites in continuous culture. *Science* 193: 673–675.
21. Radfar, A., D. Méndez, C. Moneriz, M. Linares, P. Marín-García, A. Puyet, A. Diez, and J. M. Bautista. 2009. Synchronous culture of *Plasmodium falciparum* at high parasitemia levels. *Nat. Protoc.* 4: 1899–1915.
22. Ranford-Cartwright, L. C., A. Sinha, G. S. Humphreys, and J. M. Mwangi. 2010. New synchronization method for *Plasmodium falciparum*. *Malar. J.* 9: 170.
23. León, D. L., I. Fellay, P. Y. Mantel, and M. Walch. 2017. Killing bacteria with cytotoxic effector proteins of human killer immune cells: granzymes, granulysin, and perforin. *Methods Mol. Biol.* 1535: 275–284.
24. Thiery, J., M. Walch, D. K. Jensen, D. Martinvalet, and J. Lieberman. 2010. Isolation of cytotoxic T cell and NK granules and purification of their effector proteins. *Curr. Protoc. Cell Biol.* 47: 3.37.1–3.37.29.
25. Walch, M., S. Latinovic-Golic, A. Velic, H. Sundstrom, C. Dumrese, C. A. Wagner, P. Groscurth, and U. Ziegler. 2007. Perforin enhances the granulysin-induced lysis of *Listeria* innocua in human dendritic cells. *BMC Immunol.* 8: 14.
26. Guenot, M., S. Loizon, J. Howard, G. Costa, D. A. Baker, S. Y. Mohabeer, M. Troye-Blomberg, J. F. Moreau, J. Déchanet-Merville, O. Mercereau-Puijalon, et al. 2015. Phosphoantigen burst upon plasmodium falciparum schizont rupture can distantly activate Vγ9Vδ2 T cells. *Infect. Immun.* 83: 3816–3824.
27. Aurore, V., F. Caldana, M. Blanchard, S. Kharoubi Hess, N. Lannes, P. Y. Mantel, L. Filgueira, and M. Walch. 2018. Silver-nanoparticles increase bactericidal activity and radical oxygen responses against bacterial pathogens in human osteoclasts. *Nanomedicine (Lond.)* 14: 601–607.
28. Kolber, M. A., R. R. Quinones, R. E. Gress, and P. A. Henkart. 1988. Measurement of cytotoxicity by target cell release and retention of the fluorescent dye bis-carboxyethyl-carboxyfluorescein (BCECF). *J. Immunol. Methods* 108: 255–264.
29. Mamedov, M. R., A. Scholzen, R. V. Nair, K. Cumnock, J. A. Kenkel, J. H. M. Oliveira, D. L. Trujillo, N. Saligrama, Y. Zhang, F. Rubelt, et al. 2018. A macrophage colony-stimulating-factor-producing γδ T cell subset prevents malarial parasitemic recurrence. *Immunity* 48: 350–363.e7.
30. Dunne, J., S. Lynch, C. O'Farrelly, S. Todryk, J. E. Hegarty, C. Feighery, and D. G. Doherty. 2001. Selective expansion and partial activation of human NK cells and NK receptor-positive T cells by IL-2 and IL-15. *J. Immunol.* 167: 3129–3138.
31. Inoue, S., M. Niikura, S. Mineo, and F. Kobayashi. 2013. Roles of IFN-γ and γδ T cells in protective immunity against blood-stage malaria. *Front. Immunol.* 4: 258.
32. Jenkins, M. R., and G. M. Griffiths. 2010. The synapse and cytolytic machinery of cytotoxic T cells. *Curr. Opin. Immunol.* 22: 308–313.
33. Kaul, D. K., E. F. Roth, Jr., R. L. Nagel, R. J. Howard, and S. M. Handunnetti. 1991. Rosetting of *Plasmodium falciparum*-infected red blood cells with uninfected red blood cells enhances microvascular obstruction under flow conditions. *Blood* 78: 812–819.
34. Paing, M. M., N. D. Salinas, Y. Adams, A. Oksman, A. T. Jensen, D. E. Goldberg, and N. H. Tolia. 2018. Shed EBA-175 mediates red blood cell clustering that enhances malaria parasite growth and enables immune evasion. *eLife* 7: e43224.
35. Pasini, E. M., D. van den Ierssel, H. J. Vial, and C. H. Kocken. 2013. A novel live-dead staining methodology to study malaria parasite viability. *Malar. J.* 12: 190.
36. Su, B., M. R. Bochan, W. L. Hanna, C. J. Froelich, and Z. Brahmi. 1994. Human granzyme B is essential for DNA fragmentation of susceptible target cells. *Eur. J. Immunol.* 24: 2073–2080.
37. Kataoka, T., N. Shinohara, H. Takayama, K. Takaku, S. Kondo, S. Yonehara, and K. Nagai. 1996. Concanamycin A, a powerful tool for characterization and estimation of contribution of perforin- and Fas-based lytic pathways in cell-mediated cytotoxicity. *J. Immunol.* 156: 3678–3686.
38. Ye, W., M. Chew, J. Hou, F. Lai, S. J. Leopold, H. L. Loo, A. Ghose, A. K. Dutta, Q. Chen, E. E. Ooi, et al. 2018. Microvesicles from malaria-infected red blood cells activate natural killer cells via MDA5 pathway. *PLoS Pathog.* 14: e1007298.
39. Praper, T., A. Sonnen, G. Viero, A. Kladnik, C. J. Froelich, G. Anderluh, M. Dalla Serra, and R. J. Gilbert. 2011. Human perforin employs different avenues to damage membranes. *J. Biol. Chem.* 286: 2946–2955.
40. Dotiwala, F., S. Sen Santara, A. A. Binker-Cosen, B. Li, S. Chandrasekaran, and J. Lieberman. 2017. Granzyme B disrupts central metabolism and protein synthesis in bacteria to promote an immune cell death program. *Cell* 171: 1125–1137.e11.
41. Hale, V. L., J. M. Watermeyer, F. Hackett, G. Vizcay-Barrena, C. van Ooij, J. A. Thomas, M. C. Spink, M. Harkiolaki, E. Duke, R. A. Fleck, et al. 2017. Parasitophorous vacuole poration precedes its rupture and rapid host erythrocyte cytoskeleton collapse in *Plasmodium falciparum* egress. *Proc. Natl. Acad. Sci. USA* 114: 3439–3444.
42. Hviid, L., J. A. Kurtzhals, V. Adabayeri, S. Loizon, K. Kemp, B. Q. Goka, A. Lim, O. Mercereau-Puijalon, B. D. Akanmori, and C. Behr. 2001. Perturbation and proinflammatory type activation of V delta 1(+) gamma delta T cells in African children with *Plasmodium falciparum* malaria. *Infect. Immun.* 69: 3190–3196.
43. Langhorne, J., S. Morris-Jones, L. G. Casabo, and M. Goodier. 1994. The response of gamma delta T cells in malaria infections: a hypothesis. *Res. Immunol.* 145: 429–436.

44. Bordessoule, D., P. Gaulard, and D. Y. Mason. 1990. Preferential localisation of human lymphocytes bearing gamma delta T cell receptors to the red pulp of the spleen. *J. Clin. Pathol.* 43: 461–464.
45. Chang, W. L., H. van der Heyde, D. G. Maki, M. Malkovsky, and W. P. Weidanz. 1992. Subset heterogeneity among gamma delta T cells found in peripheral blood during *Plasmodium falciparum* malaria. *Immunol. Lett.* 32: 273–274.
46. van der Heyde, H. C., M. M. Elloso, D. C. Roopenian, D. D. Manning, and W. P. Weidanz. 1993. Expansion of the CD4-, CD8- gamma delta T cell subset in the spleens of mice during non-lethal blood-stage malaria. *Eur. J. Immunol.* 23: 1846–1850.
47. Elloso, M. M., H. C. van der Heyde, J. A. vande Waa, D. D. Manning, and W. P. Weidanz. 1994. Inhibition of *Plasmodium falciparum* in vitro by human gamma delta T cells. *J. Immunol.* 153: 1187–1194.
48. Troye-Blomberg, M., S. Worku, P. Tangteerawatana, R. Jamshaid, K. Söderström, G. Elghazali, L. Moretta, M. Hammarström, and L. Mincheva-Nilsson. 1999. Human gamma delta T cells that inhibit the in vitro growth of the asexual blood stages of the *Plasmodium falciparum* parasite express cytolytic and proinflammatory molecules. *Scand. J. Immunol.* 50: 642–650.
49. Harly, C., Y. Guillaume, S. Nedellec, C. M. Peigné, H. Mönkkönen, J. Mönkkönen, J. Li, J. Kuball, E. J. Adams, S. Netzer, et al. 2012. Key implication of CD277/butyrophilin-3 (BTN3A) in cellular stress sensing by a major human γδ T-cell subset. *Blood* 120: 2269–2279.
50. Scotet, E., L. O. Martinez, E. Grant, R. Barbaras, P. Jenö, M. Guiraud, B. Monsarrat, X. Saulquin, S. Maillet, J. P. Estève, et al. 2005. Tumor recognition following Vgamma9Vdelta2 T cell receptor interactions with a surface F1-ATPase-related structure and apolipoprotein A-I. *Immunity* 22: 71–80.
51. Willcox, C. R., V. Pitard, S. Netzer, L. Couzi, M. Salim, T. Silberzahn, J. F. Moreau, A. C. Hayday, B. E. Willcox, and J. Déchanet-Merville. 2012. Cytomegalovirus and tumor stress surveillance by binding of a human γδ T cell antigen receptor to endothelial protein C receptor. *Nat. Immunol.* 13: 872–879.
52. Böttger, E., G. Multhoff, J. F. Kun, and M. Esen. 2012. *Plasmodium falciparum*-infected erythrocytes induce granzyme B by NK cells through expression of host-Hsp70. *PLoS One* 7: e33774.
53. Pongponratn, E., M. Riganti, B. Punpoowong, and M. Aikawa. 1991. Microvascular sequestration of parasitized erythrocytes in human falciparum malaria: a pathological study. *Am. J. Trop. Med. Hyg.* 44: 168–175.
54. Yañez, D. M., J. Batchelder, H. C. van der Heyde, D. D. Manning, and W. P. Weidanz. 1999. Gamma delta T-cell function in pathogenesis of cerebral malaria in mice infected with *Plasmodium* berghei ANKA. *Infect. Immun.* 67: 446–448.
55. Haque, A., H. Echchannaoui, R. Seguin, J. Schwartzman, L. H. Kasper, and S. Haque. 2001. Cerebral malaria in mice: interleukin-2 treatment induces accumulation of gammadelta T cells in the brain and alters resistant mice to susceptible-like phenotype. *Am. J. Pathol.* 158: 163–172.
56. Buffet, P. A., I. Safeukui, G. Deplaine, V. Brousse, V. Prendki, M. Thellier, G. D. Turner, and O. Mercereau-Puijalon. 2011. The pathogenesis of *Plasmodium falciparum* malaria in humans: insights from splenic physiology. *Blood* 117: 381–392.
57. Snow, R. W., J. A. Omumbo, B. Lowe, C. S. Molyneux, J. O. Obiero, A. Palmer, M. W. Weber, M. Pinder, B. Nahlen, C. Obonyo, et al. 1997. Relation between severe malaria morbidity in children and level of *Plasmodium falciparum* transmission in Africa. *Lancet* 349: 1650–1654.
58. Barman, H., M. Walch, S. Latinovic-Golic, C. Dumrese, M. Dolder, P. Groscurth, and U. Ziegler. 2006. Cholesterol in negatively charged lipid bilayers modulates the effect of the antimicrobial protein granulysin. *J. Membr. Biol.* 212: 29–39.
59. Maguire, P. A., and I. W. Sherman. 1990. Phospholipid composition, cholesterol content and cholesterol exchange in *Plasmodium falciparum*-infected red cells. *Mol. Biochem. Parasitol.* 38: 105–112.
60. Tokumasu, F., G. Crivat, H. Ackerman, J. Hwang, and T. E. Wellems. 2014. Inward cholesterol gradient of the membrane system in P. falciparum-infected erythrocytes involves a dilution effect from parasite-produced lipids. *Biol. Open* 3: 529–541.
61. Kapelski, S., M. de Almeida, R. Fischer, S. Barth, and R. Fendel. 2015. Antimalarial activity of granzyme B and its targeted delivery by a granzyme B-single-chain Fv fusion protein. *Antimicrob. Agents Chemother.* 59: 669–672.
62. Hermsen, C. C., Y. Konijnenberg, L. Mulder, C. Loé, M. van Deuren, J. W. van der Meer, G. J. van Mierlo, W. M. Eling, C. E. Hack, and R. W. Sauerwein. 2003. Circulating concentrations of soluble granzyme A and B increase during natural and experimental *Plasmodium falciparum* infections. *Clin. Exp. Immunol.* 132: 467–472.
63. Burel, J. G., S. H. Apte, J. S. McCarthy, and D. L. Doolan. 2016. *Plasmodium* vivax but not *Plasmodium falciparum* blood-stage infection in humans is associated with the expansion of a CD8+ T cell population with cytotoxic potential. *PLoS Negl. Trop. Dis.* 10: e0005031.
64. Junqueira, C., C. R. R. Barbosa, P. A. C. Costa, A. Teixeira-Carvalho, G. Castro, S. Sen Santara, R. P. Barbosa, F. Dotiwala, D. B. Pereira, L. R. Antonelli, et al. 2018. Cytotoxic $CD8^+$ T cells recognize and kill plasmodium vivax-infected reticulocytes. *Nat. Med.* 24: 1330–1336.

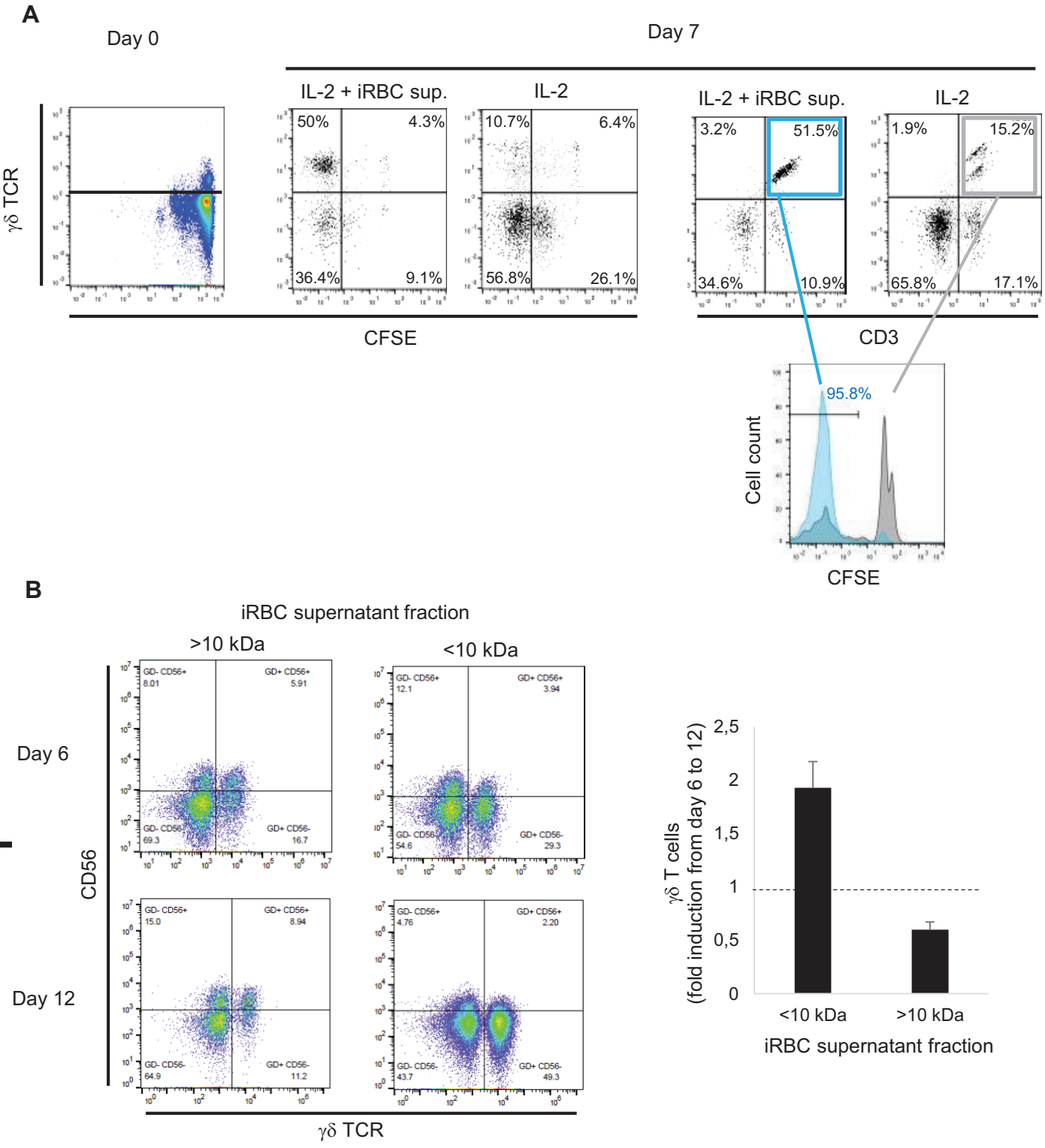

Supplementary Figure 1. Proliferation of γδ T cells upon stimulation with iRBC supernatant and IL-2.
(**A**) Peripheral blood mononuclear cells (PBMCs) were labeled with CFSE and then activated with culture supernatant of parasitized red blood cells (iRBCs) and IL-2 or IL-2 alone for 7 days. At days 0 and 7 of the activation, the cells were stained with anti-CD3 and anti-γδ TCR for analysis by flow cytometry. Representative cytometry plots out of three independent experiments are shown. (**B**) PBMCs were activated with IL-2 and iRBCs supernatant, previously fractionated using 10 kDa molecular cut-off spin filters. Representative cytometry plots and fold fold induction of γδ T cells during the activation from day 6 to day 12 in two donors are presented.

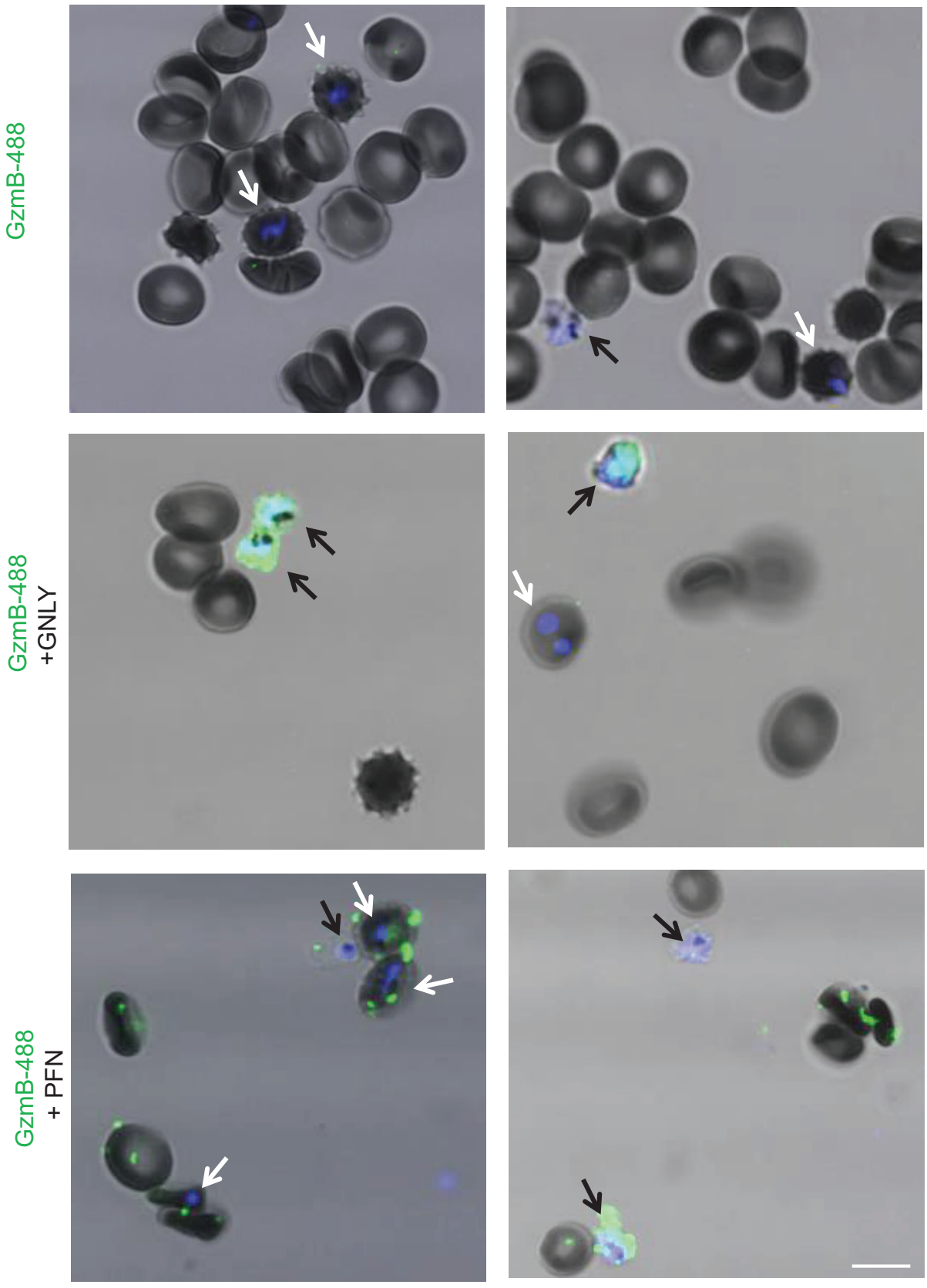

Supplementary Figure 2. Transfer of GzmB in iRBCs.
Non-synchronized iRBCs cultures were treated with Alexa Fluor 488-labeled GzmB in combination with PFN or GNLY for 20 minutes before fixation, counterstaining with Hoechst to visualize DNA and assessment by confocal microscopy. Late stages are indicated by black arrows and early stages by white arrows. Scale bar = 10 mm.